Journal of Power Sources 193 (2009) 899–907

Contents lists available at ScienceDirect

Journal of Power Sources

journal homepage: www.elsevier.com/locate/jpowsour

Review

Fuzzy logic control of stand-alone photovoltaic system with battery storage

S. Lalouni [a], D. Rekioua [a,*], T. Rekioua [a], E. Matagne [b]

[a] Department of Electrical Engineering, University of Bejaia, Bejaia, Algeria
[b] Laboratory of Electrical Engineering and Instrumentation; UCL, Louvain La Neuve, Belgique

ARTICLE INFO

Article history:
Received 5 February 2009
Received in revised form 15 April 2009
Accepted 16 April 2009
Available online 23 April 2009

Keywords:
Photovoltaic systems
Maximum power point tracker
Fuzzy logic controller (FLC)
DC–DC converter
Storage battery

ABSTRACT

Photovoltaic energy has nowadays an increased importance in electrical power applications, since it is considered as an essentially inexhaustible and broadly available energy resource. However, the output power provided via the photovoltaic conversion process depends on solar irradiation and temperature. Therefore, to maximize the efficiency of the photovoltaic energy system, it is necessary to track the maximum power point of the PV array. The present paper proposes a maximum power point tracker (MPPT) method, based on fuzzy logic controller (FLC), applied to a stand-alone photovoltaic system. It uses a sampling measure of the PV array power and voltage then determines an optimal increment required to have the optimal operating voltage which permits maximum power tracking. This method carries high accuracy around the optimum point when compared to the conventional one. The stand-alone photovoltaic system used in this paper includes two bi-directional DC/DC converters and a lead-acid battery bank to overcome the scare periods. One converter works as an MPP tracker, while the other regulates the batteries state of charge and compensates the power deficit to provide a continuous delivery of energy to the load. The Obtained simulation results show the effectiveness of the proposed fuzzy logic controller.

Contents

1. Introduction

As conventional energy sources are dwindling fast with a consequent rise in cost, considerable attention is being paid to other alternative sources. Solar energy which is free and abundant in most parts of the world has proven to be an economical source of energy in many applications. The photovoltaic process is a technology in which radiant energy from the sun is converted to direct current (DC) electricity. The photovoltaic process is completely solid state and self contained. There are no moving parts and no materials are consumed or emitted. The PV array has a unique operating point that can supply maximum power to the load. This point is called the maximum power point (MPP). The locus of this point has a non-linear variation with solar irradiation and the cell temperature. Thus, in order to operate the PV array at its optimum point, the system must contain impedance adapter. It is in fact a DC or AC converter, driving by classic or advanced controller [1,2].

Many methods and controllers have been widely developed and implemented to track the maximum power point (MPP). A look-up table based on a microcomputer is employed in Ref. [3]. It uses a database that includes parameters and data such as PV generator's typical curves. In Ref. [4], curve-fitting method is used, where the non-linear characteristic of PV generator is modelled using

* Corresponding author. Tel.: +213 34215006; fax: +213 34215005.
E-mail addresses: lalouni_sofia@yahoo.fr (S. Lalouni), dja_rekioua@yahoo.fr (D. Rekioua).

0378-7753/$ – see front matter © 2009 Elsevier B.V. All rights reserved.
doi:10.1016/j.jpowsour.2009.04.016

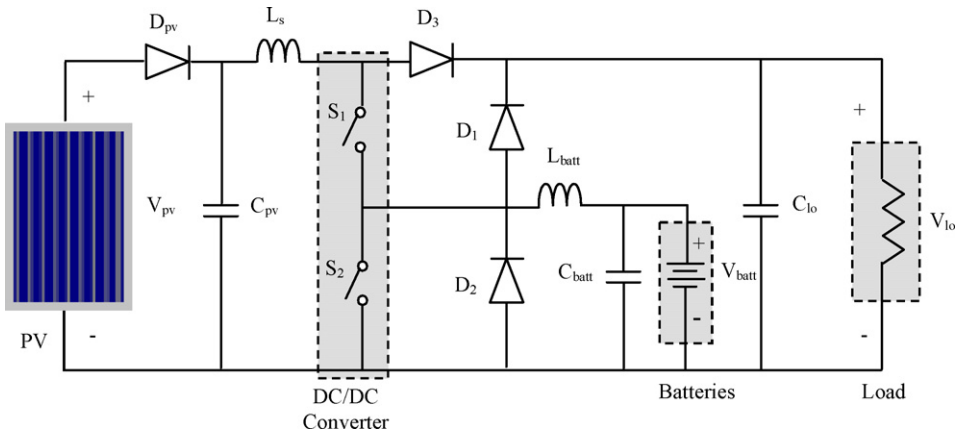

Fig. 1. Structure of a stand-alone PV system.

mathematical equations or numerical approximations. These two algorithms require a large memory capacity, for calculation of the mathematical formulations and data storing. References [5,6] use pilot panels to perform MPP tracking. The optimum current/voltage presents a linear dependency with short circuit current/open circuit voltage, respectively. These methods are apparently simple and economical, but they cannot be adapted to changing environmental conditions. Most control schemes use the P&O technique, which is based on iterative algorithms, because it is easy to implement but the oscillation problem is unavoidable [7–11]. A conductance incremental method requires complex control circuit [11]. The two last methods have some disadvantages such as high cost, complexity and instability.

Other intelligent based control schemes have been introduced (fuzzy logic, neural network) [11–22]. The inputs of the fuzzy logic controllers are an error and an error variation, the output is a duty cycle or its variation. The fuzzy controller introduced in [12–14] uses dP_{pv}/dI_{pv} and its variations $\Delta(dP_{pv}/dI_{pv})$ as inputs, computes MPPT converter duty cycle in the first reference and the variation of the last one in the two other references. Whereas, the fuzzy tracker in [15–17] considers variation of duty cycle as an output but replaces dP_{pv}/dI_{pv} by the variation of panel power. The linguistic variables assigned to output for different combinations of inputs are based on the power converter being used. In Ref. [13], a FLC developed is inadequate when the operating conditions change in a wide range. The adaptive FLC [13] and the FCM [14] approach which is a hybrid modelling methodology, exploiting the characteristics of fuzzy logic and neural networks theories, presents much high computation.

In our case, inputs parameters used to generate the optimal reference voltage which correspond to a maximum power are power variation (ΔP_{pv}) and voltage variation (ΔV_{pv}). As output, it determines the optimal increment which must be added to the operating voltage for tracking the MPP in order to assure fast and fine tracking. Contrary to the conventional perturbation and observation (P&O) algorithm which uses constant perturbation to determine the operating voltage that produces oscillations of the operation point around the MPP at a steady state. This controller is suitable for any DC/DC topology and gives robust performances under variations in environmental operating conditions and load.

The performance of the new FLC is tested using stand-alone PV system for various operational conditions, such as changing solar radiance, temperature and load. The paper is organized as follows. In Section 2, we present the stand-alone photovoltaic system with battery storage used. Mathematical relations between the essential variables of a PV system are presented in Section 3. These relations are necessary for simulating its operation under different solar radiance and temperature. Due to the fluctuation nature of photovoltaic energy source, batteries are added in order to ensure continuous power-flow. The storage battery model used is presented with obtained measurement results. In order to track the MPP of a PV system, an MPPT method, which is based on a fuzzy controller, is developed in Section 4, while in Section 5, the obtained simulation results, using the MATLAB®-SIMULINK® package [23] are given and interpreted. These last runs based on sampled local climatic data of one month. Finally, Section 6 concludes the work.

2. System description

Fig. 1 shows a synoptic scheme of the PV-stand-alone photovoltaic system used in this paper. It includes a PV array of 110 W, two DC/DC converters. The first allows maximum utilization of the photovoltaic array, while the second, and via its bi-directional nature, performs two tasks: The battery's state-of-charge (SOC) control and a power-flow controller to ensure a continuous delivery of energy to the load whatever environmental conditions variations and load disturbances. Depending on environmental conditions, the stand-alone PV system operates in one of the two following modes of operation:

- Batteries charge mode: in this mode the PV arrays generate sufficient energy to feed the load and charge battery.
- Power compensation mode: in this mode the energy available in PV arrays is not sufficient to supply the load, the battery bank supplements the energy required by the load. A particular operation in this mode occurs when there is no available energy at PV arrays. In this case, the battery bank supplies full load current. The converter displayed is a boost one; it amplifies the voltage of battery to produce the load voltage.

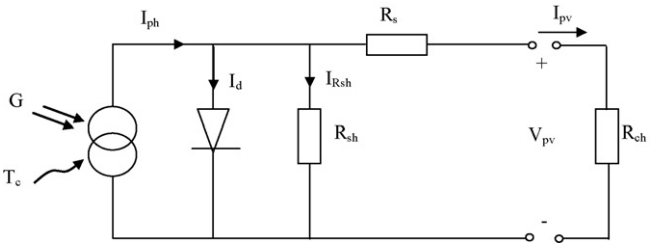

Fig. 2. Equivalent circuit of solar cell.

3. Modeling of the proposed system

3.1. Model of PV Array

The PV generator is a non-linear device and is usually described by its *I–V* characteristics and by the equivalent circuit. Various mathematical models of photovoltaic generators were developed to represent this non-linear behaviour which results from the semiconductors junctions. In the present work, the called "Four-Parameter Model" which is widely used by different software is used [24]. It predicts with success the performance of single crystal and polycrystalline PV arrays: Fig. 2

The PV array equivalent circuit current I_{pv} can be expressed as a function of the PV array voltage V_{pv}:

$$I_{pv} = I_{sc}\left\{1 - K_1\left[\exp K_2 V_{pv}^{m} - 1\right]\right\} \quad (1)$$

where the coefficients K_1, K_2 and m are defined as [24]:

$$K_1 = 0.01175$$

$$K_2 = \frac{K_4}{V_{oc}^{m}} \quad (2)$$

$$K_3 = \ln\left[\frac{I_{sc}(1+K_1) - I_{mpp}}{K_1 I_{sc}}\right] \quad (3)$$

$$K_4 = \ln\left[\frac{1+K_1}{K_1}\right] \quad (4)$$

Table 1
Parameter of the PV panel SIEMENS SM 110-24.

P_{PV}	110 W
I_{mpp}	3.15 A
V_{mpp}	35 V
I_{sc}	3.45 A
V_{oc}	43.5 V
α_{sc}	1.4 mA/°C
β_{oc}	−152 mV/°C
P_{mpp}	110 W

$$m = \frac{\ln\left[K_3/K_4\right]}{\ln\left[V_{mpp}/V_{oc}\right]} \quad (5)$$

where: V_{mpp}: maximum power point voltage; $V_{oc:}$ open circuit voltage; $I_{mpp:}$ maximum power point current; I_{sc}: short circuit current.

The *I–V* curve is essentially affected by the variation of two inputs: the solar irradiance and the array temperature. The adaptation of Eq. (1) for different levels of solar insolation and temperature can be handled by the following equations [24]:

$$\Delta T_c = T_c - T_{stc} \quad (6)$$

$$\Delta I_{pv} = \alpha_{sc}\left(\frac{G}{G_{stc}}\right)\Delta T_c + \left(\frac{G}{G_{stc}} - 1\right) I_{sc,stc} \quad (7)$$

$$\Delta V_{pv} = -\beta_{oc}\Delta T_c - R_s \Delta I_{pv} \quad (8)$$

where: α_{sc}: current temperature coefficient; β_{oc}: voltage temperature coefficient; R_s: series cell resistance.

Fig. 3. PV array structure, controller, inverter and battery.

The new values of the photovoltaic voltage and current are given by:

$$V_{pv,new} = V_{pv} + \Delta V_{pv} \quad (9)$$

$$I_{pv,new} = I_{pv} + \Delta I_{pv}$$

Table 1 shows PV panel's data at STC for a SM 110-24 panel which is used in simulations. The PV system in Fig. 3 is located at the University of Bejaia (Algeria).

The curves power–voltage $P_{pv}(V_{pv})$ and current–voltage $I_{pv}(V_{pv})$ of the photovoltaic panel, are carried out by varying the load's resistance for three levels of irradiance and temperature (Fig. 4a and b). The experimental characteristics obtained are compared to the simulation characteristics for the same operating conditions ($G = 450\,W\,m^{-2}$, $T_c = 25\,^{\circ}C$; $G = 650\,W\,m^{-2}$, $T_c = 33\,^{\circ}C$; $G = 900\,W\,m^{-2}$, $T_c = 35\,^{\circ}C$).

From the current and power characteristics (Fig. 4), the non-linear nature of the PV array is apparent. Therefore, an MPPT algorithm must be incorporated to force the system to always operate at the maximum power point (MPP).

3.2. Electrical model of Battery

The system of storage is composed of two lead-acid batteries of 12 V, 92 Ah inter-connected in series to have 24 V. In practice, the determination of the batteries' impedances is often made on stationary behaviour. The basic principle is to impose on the battery an excitation in voltage or current in order to deduce in response to this excitation, an Ohmic representation of its internal state [25]. Measurement at weak frequency gives more information on electrochemical operation because the internal kinetics of the battery has thus the time to react to the imposed disturbance. In order to determine the internal impedance of the battery (12 V, 92 Ah) for one state of charge of the battery, we superimpose an alternate sinusoidal signal of 50 Hz frequency to the continuous component of the battery according to following steps:

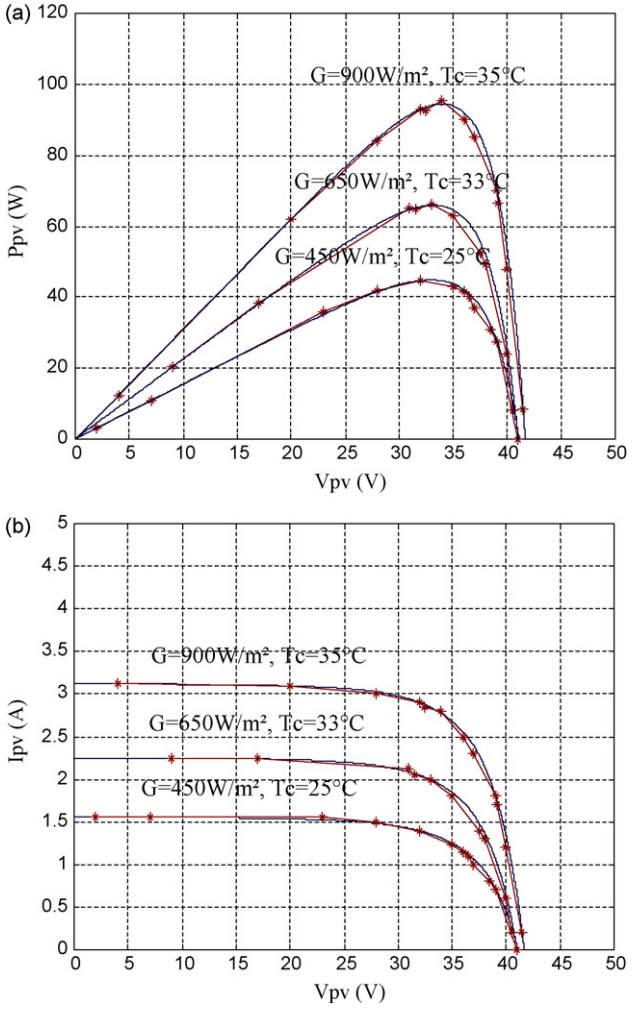

Fig. 4. (a) Experimental and simulation curves P_V (V_{PV}). (b) Experimental and simulation curves I_{PV} (V_{PV}).

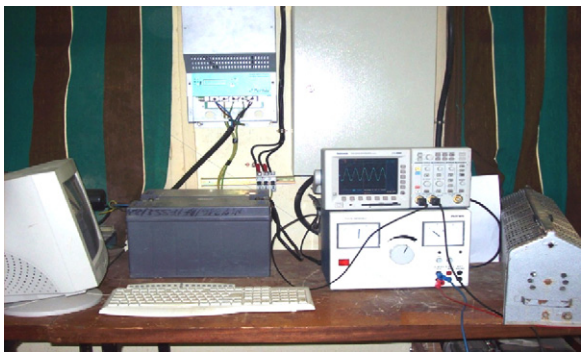

Fig. 5. Circuit measurement of battery impedances.

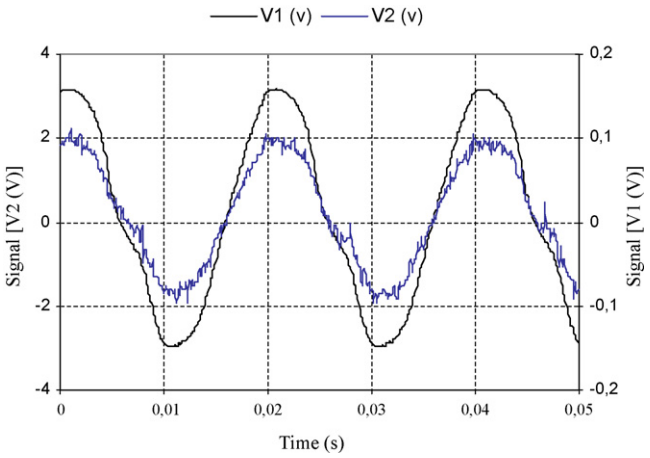

Fig. 6. Signals measured V_1 and V_2.

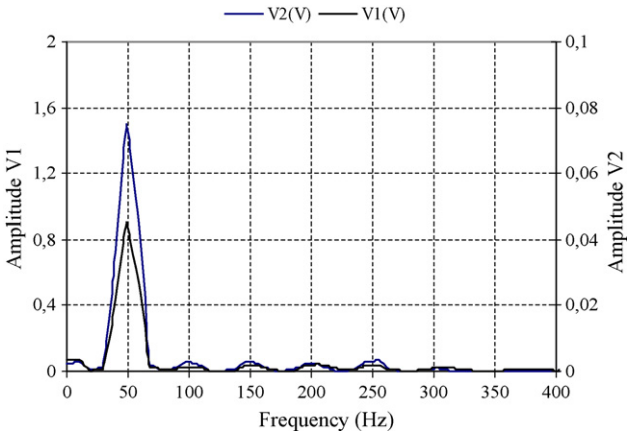

Fig. 7. Harmonic spectrum of signals V_1 and V_2.

Table 2
Fuzzy rule table.

$\Delta V_{pv} \backslash \Delta P_{pv}$	BN	MN	SN	Z	SP	MP	BP
BN	BP	BP	MP	Z	MN	BN	BN
MN	BP	MP	SP	Z	SN	MN	BN
SN	MP	SP	SP	Z	SN	SN	MN
Z	BN	MN	SN	Z	SP	MP	BP
SP	MN	SN	SN	Z	SP	SP	MP
MP	BN	MN	SN	Z	SP	MP	BP
BP	BN	BN	MN	Z	MP	BP	BP

Table 3
Simulation parameters.

PV power P_{mpp}	110 W
Load power P_{ch}	70 W
Load voltage V_{ch}	48 V
Battery voltage V_{batt}	24 V
Inductor L_s	1 mH
Inductor L_{batt}	1 mH
Capacitor C_{pv}	1.2 mF
Capacitor C_{batt}	330 μF
Capacitor C_{ch}	470 μF

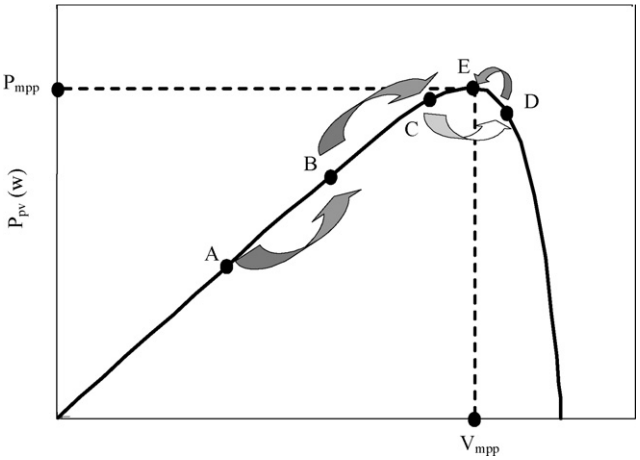

Fig. 8. Principle of operation of the MPPT fuzzy controller.

We close the battery on a circuit including a variable resistance, limitation (15.8 Ω, 10 A), a shunt (250 V, 10 A) a current sensor, composed by a series resistance (250 V, 10 A) and a source of alternating voltage (0–36 V, 20 A). The measurement system (Fig. 5) is developed.

We measure two voltages using an oscilloscope: the voltage at the shunt terminals which is a direct picture of the current circulating in the circuit and the battery voltage. The ratio of these two voltages and their phase-shift provides the absolute value of the internal impedance of the battery.

Measures are carried out by a digital oscilloscope (Tektronix TDS3032, 300 MHz). These digital measurements are then transferred to a computer for analysis.

Fig. 6 presents the signals recovered by Excel. The signal (V_1) is a direct image of the measurement AC current (conversion factor: 25 V = 1 A) while the second signal represents the resulting voltage on the battery's sides.

We remark a capacitance character of the battery to this measurement frequency. An analysis by Fourier transform is applied to the signals of (Fig. 6) and confirms well the fundamental frequency of 50 Hz (Fig. 7).

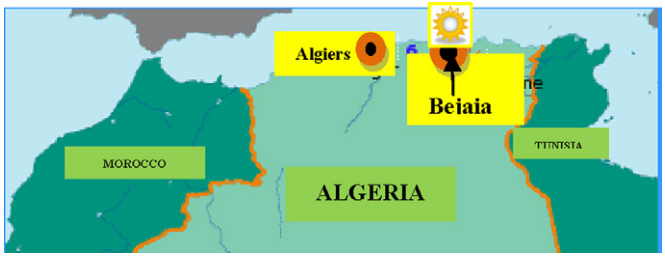

Fig. 10. Géographical situation of Bejaia.

The battery behaves as a complex impedance Z_{batt} with a resistance R_{batt} and a reactance X_{batt} to this disturbance.

$$Z_{batt} = R_{batt} - jX_{batt} \quad (10)$$

From the module of Z_{batt} and the phase-shift, we can deduce the real part R_{batt} and imaginary X_{batt} of the impedance for a state of charge. The obtained values are: R_{batt} = 0.756 Ω, X_{batt} = 0.072 Ω and C_{batt} = 44.2 mF. These values change according to the state of charge of the battery.

4. The fuzzy MPPT controller

The proposed FLC measures the PV array characteristics and then perturbs the operating voltage by an optimal increment ($\Delta V_{pv,ref}$) and the resulting PV power change. The power variation (ΔP_{pv}) is either in the positive direction or in the negative one. The value of (ΔP_{pv}) can also be small or large. From these judgements, the reference photovoltaic voltage variation ($\Delta V_{pv,ref}$) is increased or decreased in a small or respectively large way in the direction which makes it possible to increase the power P_{pv}. The control rules are indicated in Table 2 with (ΔP_{pv}) and (ΔV_{pv}) as inputs, while ($\Delta V_{pv,ref}$) represents the output. These inputs and output variables are expressed in terms of linguistic variables (such as BN (big nega-

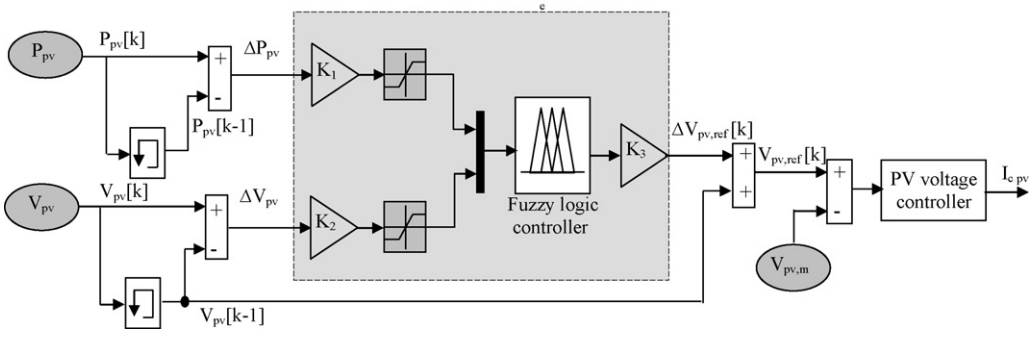

Fig. 9. Structure of MPPT fuzzy controller.

tive), MN (means negative), SN (small negative), Z (zero), SP (small positive), MP (means positive), and BP (big positive)).

From these linguistic rules, the FLC proposes a variation of the reference voltage $\Delta V_{pv,ref}$ according to Eqs. (11–13).

$$\Delta P_{pv} = P_{pv}[k] - P_{pv}[k-1] \tag{11}$$

$$\Delta V_{pv} = V_{pv}[k] - V_{pv}[k-1] \tag{12}$$

$$V_{pv,ref}[K] = V_{pv}[k-1] + \Delta V_{pv,ref}[k] \tag{13}$$

where $P_{pv}[k]$ and $V_{pv}[k]$ are the power and voltage of the photovoltaic generator at sampled times (k), and $V_{pv,ref}[k]$ the instant of reference voltage. Fig. 8 gives an example of a track in the $P_{pv}(V_{pv})$ plan for a constant irradiance and temperature.

If a great increase in the voltage V_{pv} involves a great increase in the power $P_{pv,}$ the reference voltage $V_{pv,ref}$ will continue to strongly increase (point A to B or point B to C). If a great increase in the voltage V_{pv} involves a reduction in the power P_{pv} (point C to D), the reference voltage $V_{pv,ref}$ the voltage will decrease to obtain a fast increase in the power P_{pv}. Contrary, if a reduction in the voltage V_{pv} involves a weak increase in the power P_{pv} then we get closer to the optimal reference voltage and this is the beginning of the stabilization as shown in Fig. 8. When solar radiation and temperature varies, the same types of rules are applied to track the maximum power point. The fuzzy logic controller structure is show in Fig. 9.Where K_1, K_2 and K_3 are adaptive gains.

The bloc fuzzy logic controller includes three functional blocks: fuzzification, fuzzy rule algorithm, and defuzzification.

The membership functions of inputs variables ΔP_{pv} and ΔV_{pv} are triangular and have seven fuzzy subsets. Seven fuzzy subsets are also considered for the output variable $\Delta V_{pv,ref}$. The control rules

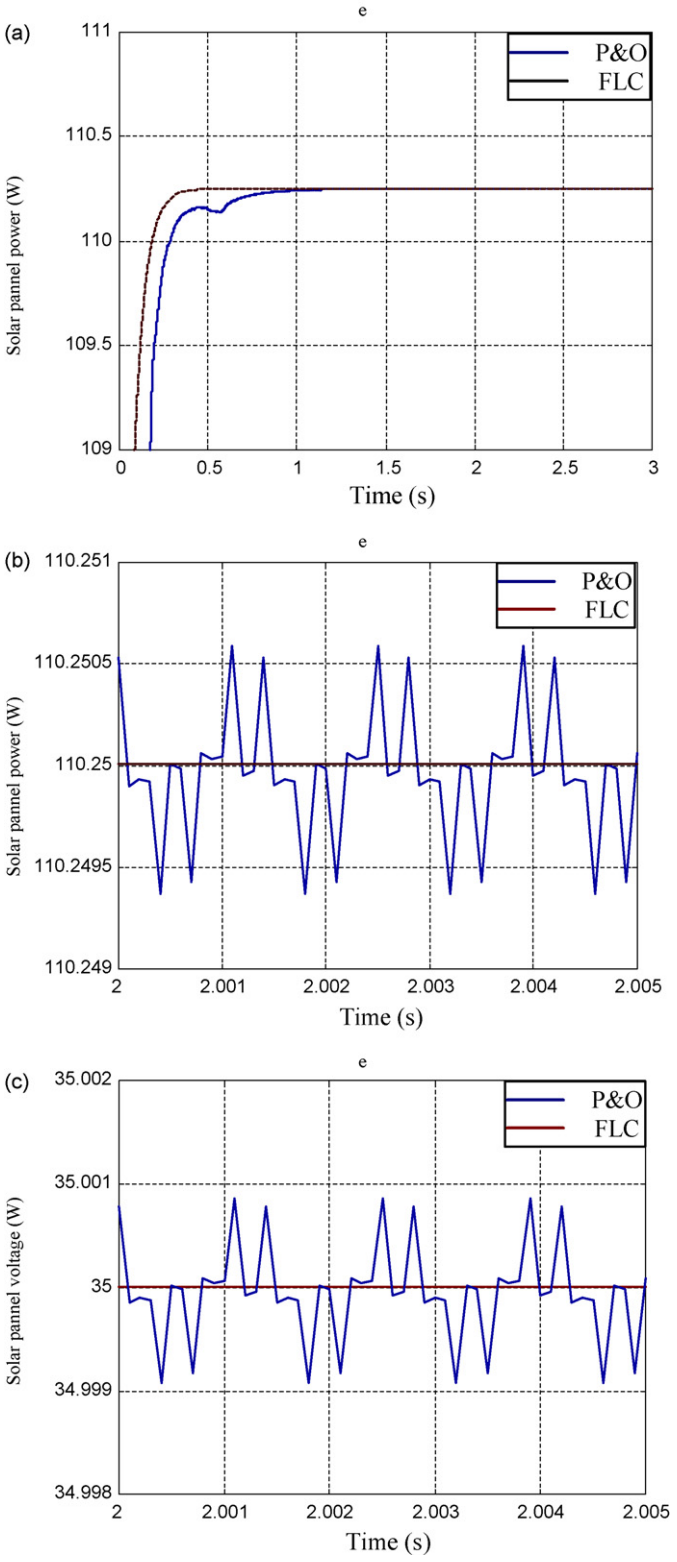

Fig. 11. (a) Transitional state of solar panel power. (b) Waveform in steady state of the solar panel power. (c) Waveform in steady state of solar panel voltage.

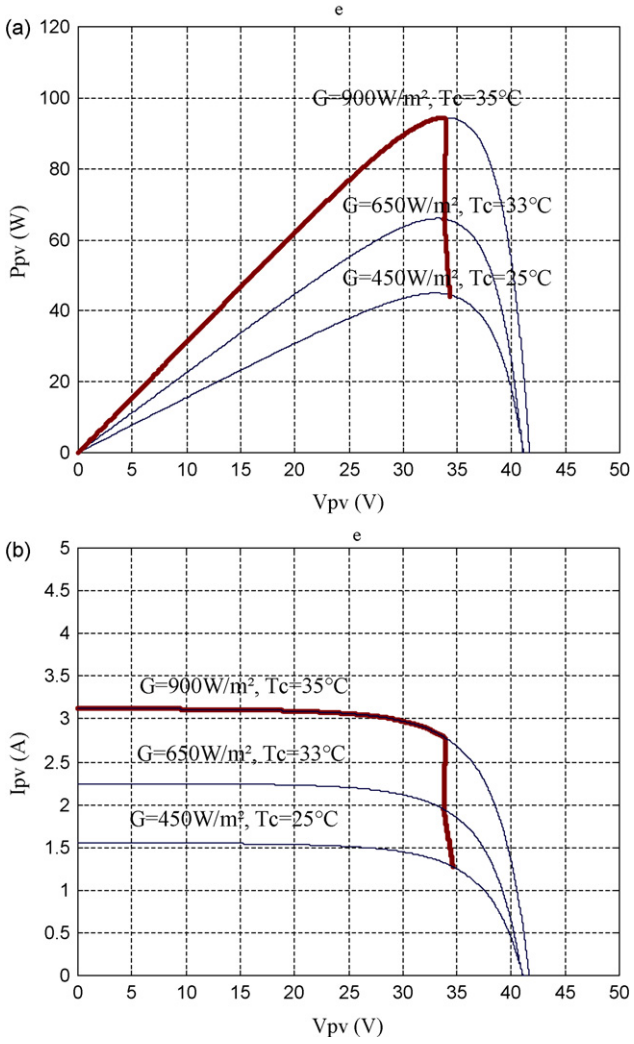

Fig. 12. (a) Power–voltage characteristic of a PV array. (b) Current–voltage characteristic of a PV array for different irradiance for different irradiance.

are indicated in Table 2 with ΔP_{pv} and ΔV_{pv} as inputs and $\Delta V_{pv,ref}$ as the output. The fuzzy inference is carried out by using Sugeno's method [26], and the defuzzification uses the centre of gravity to compute the output of this FLC.

As explained previously, the FLC optimises the reference voltage ($V_{pv,ref}$) for maximum power tracking. This voltage represents a positive input (reference) of the PI controller, which performs the voltage control in steady state. The PI loop operates with a fast rate and provides fast response and overall system stability [27].

5. Numerical simulation

The proposed system is composed of photovoltaic panel of 110 W, two storage batteries of 12 V, 92 Ah and output resistive power P_{lo} of 70 W. Various simulations evaluate the performances of the system. The various parts of the system (photovoltaic panel, DC/DC converter, battery and load), are modelled by separate blocks then related in a coherent way, while the MPPT is controlled by the proposed fuzzy logic controller (FLC). The voltage load is controlled by a PI regulator to maintain it at a constant value of 48 V. The system components of Fig. 1 are used in the simulation and its parameters are described in Table 3.

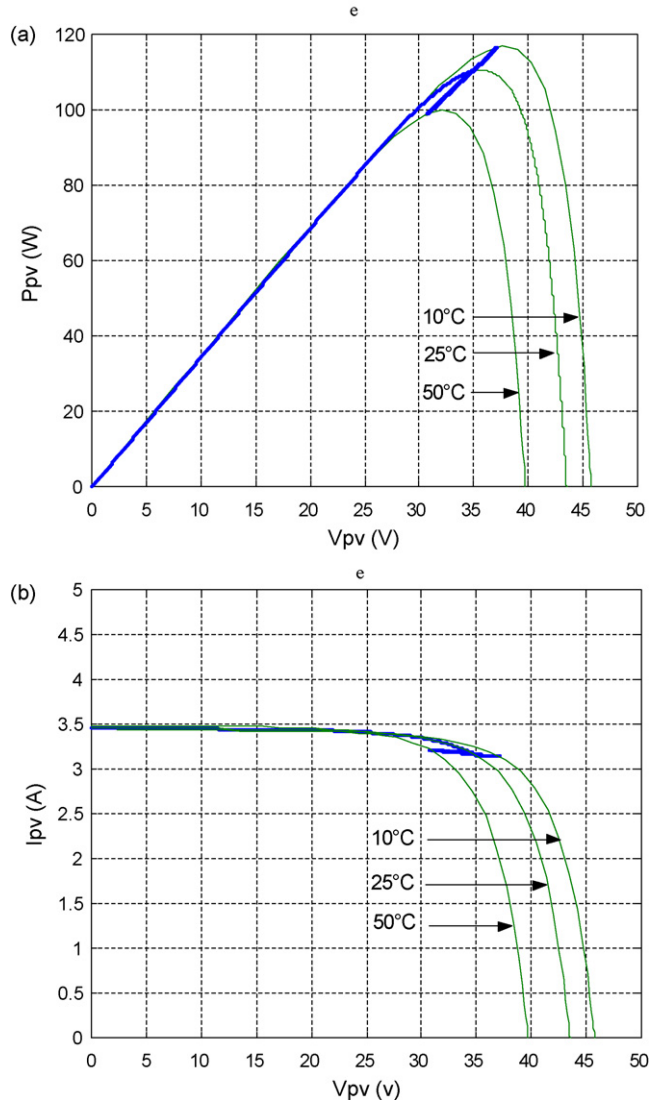

Fig. 13. (a) Power–voltage characteristic of a PV array. (b) Current–voltage characteristic of a PV array for different temperature for different temperature.

In the following simulations, the irradiance level and the cell temperature are considered to vary as:

- Solar radiation level G changes from 900 to 450 W m^{-2} and temperature T_c changes from 35 to 25 °C.
- Temperature (T_c) changes from 10 to 50 °C for constant solar radiation of 1000 W m^{-2}.
- Operation of the system for variations of solar radiation and temperature measured during one month (April 2007), at the university of Bejaia (36°43′N 5°04′E 2 m), which is a coastal city of North East of Algeria (Fig. 10).

In order to test the robustness of the proposed algorithm, simulation results were carried out using the conventional (P&O) method under the same operating conditions.

Fig. 11 presents solar panel power (P_{pv}) and solar panel voltage (V_{pv}) for the two MPPT controllers (P&O and FLC). The fuzzy logic controller (FLC) gives us a fast response since it reaches its optimal value at 0.425 s compared to perturbation and observation P&O method which requires much time to track the MPP (1.05 s) and presents oscillations around the operating point at a steady state. The FLC allows reduction not only in the convergence time to track the MPP, but also in the fluctuation of power in steady state, as it is clearly presented in Fig. 11.

The PV characteristics using FLC and the theoretical PV array characteristics are illustrated in Fig. 12a and b for variations in solar radiation level and temperature. The decrease of the solar radiation implies a decrease of the PV power. Then, the FLC determines

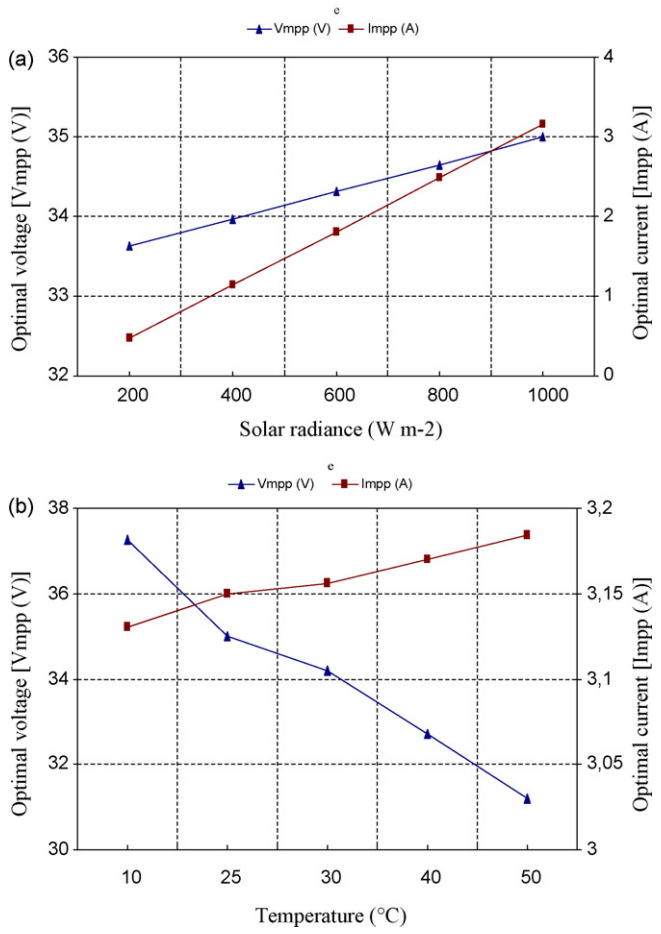

Fig. 14. (a) Optimal voltage and current of PV array. (a) Optimal voltage and current of PV array for different irradiance level with fuzzy logic controller for different temperature with fuzzy logic controller.

continuously the optimal voltage which gives us maximum power corresponding to this solar radiation. In Fig. 13a and b„ the PV array characteristics for variations in temperature (T_c) at constant solar radiation are given. The MPP of a PV array varies according to temperature and/or solar radiation variations. The FLC can drive quickly the system to the new MPP when an abrupt change of the MPP occurs. From the simulations results, it is clear that the operating point of this system operate closer to a maximum power point for variations in solar radiation and temperature. Fig. 14a and b shows the relationship between solar radiance, temperature and optimal PV array voltage V_{mpp} and current I_{mpp}.

In order to study the system's performance during a certain period of time with the proposed fuzzy logic controller (FLC), we use the experimental solar radiation and temperature data of

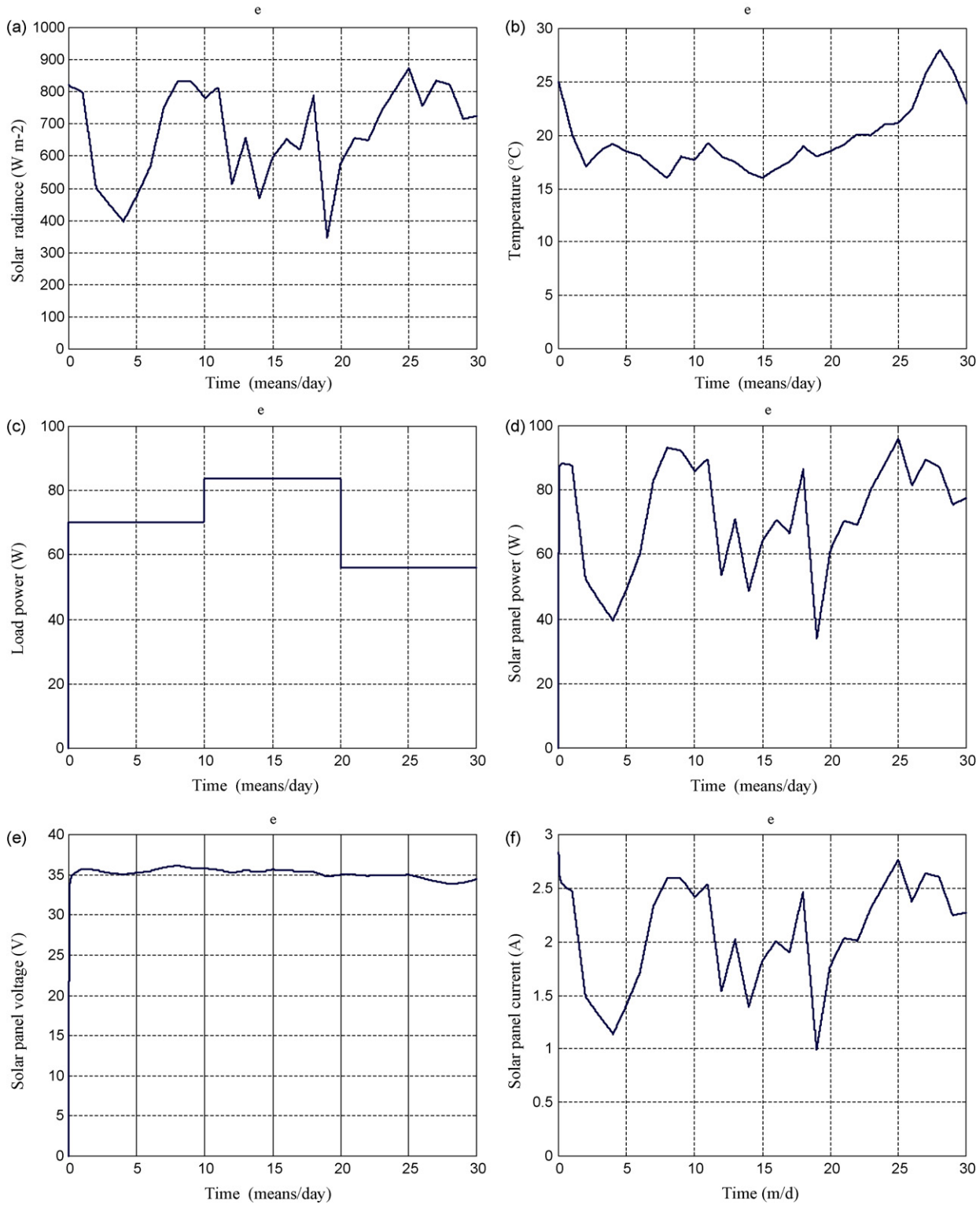

Fig. 15. (a) Measured solar radiance. (b) Measured temperature. (c) Load power. (d) Solar panel power. (e) Solar panel voltage. (f) Solar panel current. (g) Batteries current. (h) Load voltage.

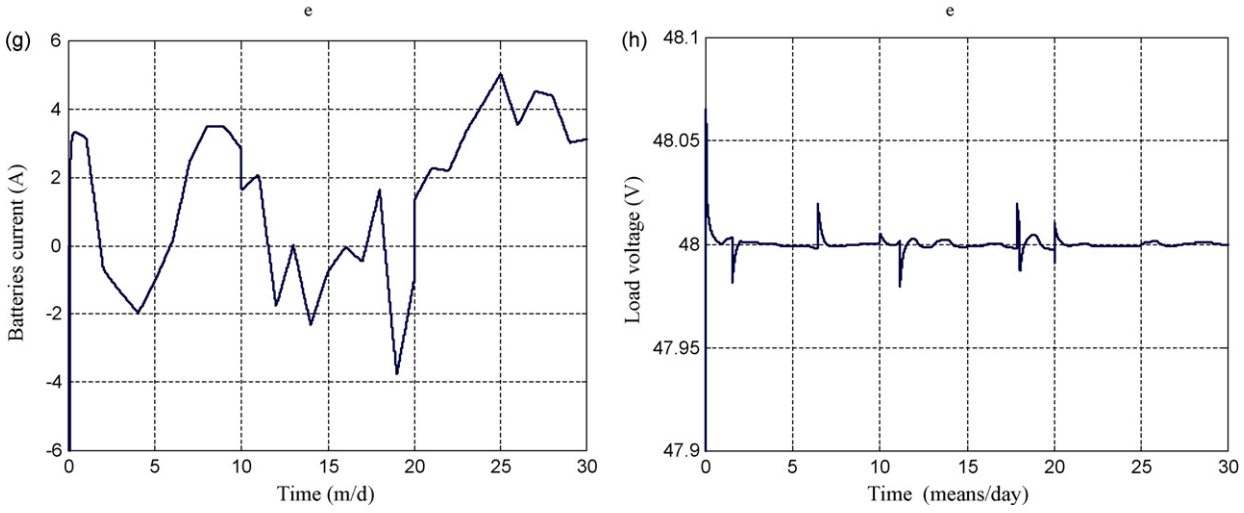

Fig. 15. (*Continued*).

means/day which are recorded at the University of Bejaia in April 2007 and given in Fig. 15a and b. The solar radiation varies up from 347 to 873 W m^{-2} and temperature varies up from 16 to 28 °C. In Fig. 15c, the load power variation P_{lo} is shown (±20% of P_{lo}). The step's profile is used to express the operating modes of the stand-alone PV system (batteries charge mode and power compensation mode).

In Fig. 15d, the maximum power tracked from the PV array is shown. The corresponding optimal voltage $V_{pv,ref}$ obtained from the fuzzy logic controller is represented in Fig. 15e. The FLC measures instantaneously PV voltage and current variations and determines quickly the optimal increment required to have the operating voltage for tracking the MPP even when the operating environmental conditions change rapidly and in a wide range. The photovoltaic current I_{pv} develops according to the variations of solar radiation (Fig. 15f). Fig. 15g, shows batteries current I_{batt}. When PV power is greater than load's power, the batteries will charge (batteries charge mode). During periods of insufficient generation, the battery bank postpones its recharge cycle and supplements the generation at the expense of its stored energy (power compensation mode). In Fig. 15h, we can see the load's voltage, it is well controlled to keep it at a constant value of 48 V whatever the environmental conditions and the load change; the PI regulator rejects these disturbances.

6. Conclusion

A novel method for maximum power point tracking was presented in this paper based on fuzzy logic theory. The proposed controller is used to speed-up the procedure of reaching the accurate maximum power point of a photovoltaic array under changing environmental conditions. The FLC adjust appropriately the optimal increment's magnitude of voltage required for reached the optimum operating voltage (tracking the MPP). The method presents very good results, where the PV system is continuously operating at the maximum power point with fast and fine tracking regardless of the weather variations, when compared to with the conventional method. In addition, we have determined an experimental battery model by superimposing an alternating sinusoidal signal of 50 Hz to the continuous component of the battery. We deduce its capacitance behaviour to this measurement frequency. The robustness of the FLC was tested via various variations of solar radiation and temperature. The obtained results demonstrate the flexibility nature of the FLC controller against climatic variations, and confirm the effectiveness of the developed method.

References

[1] S. Yuvarajan, D. Yu, S. Xu, J. Power Sources 135 (1–2) (2004) 327–331.
[2] Z.D. Zhong, H.B. Huo, X.J. Zhu, G.Y. Cao, Y. Ren, J. Power Sources 176 (1) (2008) 259–269.
[3] H.E.-S.A. Ibrahim, F.F. Houssiny, H.M.Z. El-Din, M.A. El-Shibini, Proceedings of the IEEE International Conference on Fuzzy Systems FUZZ IEEE'99, vol. 1, 1999, pp. 406–411.
[4] K. Nishioka, N. Sakitani, K. Kurobe, Y. Yamamoto, Y. Ishikawa, Y. Uraoka, T. Fuyuki, J. Appl. Phys. 42 (2003) 7175–7179.
[5] M.A.S. Masoum, H. Dehbonei, E.F. Fuchs, IEEE Trans. Energy Convers. 17 (4) (2002) 514–522.
[6] T. Noguchi, S. Togashi, R. Nakamoto, IEEE Trans. Ind. Electron. 49 (1) (2002) 217–223.
[7] L.J.L. Santos, F. Antunes, A. Chehab, C. Cruz, Solar Energy 80 (7) (2006) 772–778.
[8] Z. Salameh, D. Taylor, Solar Energy 44 (1) (1990) 57–61.
[9] Ch. Hua, J. Lin, Ch. Shen, IEEE Trans. Ind. Electron. 45 (1) (1998) 99–107.
[10] J.-A. Jiang, T.-L. Huang, Y.-T. Hsiao, C.-H Chen, Tamkang J. Sci. Eng. 8 (2) (2005) 147–153.
[11] V. Salas, E. Olias, A. Barrado, A. Lazaro, Sol. Energy Mater. Sol. Cells 90 (11) (2006) 1555–1578.
[12] C.-Y. Won, D.-H. Kim, S.-C. Kim, W.-S. Kim, H.-S. Kim, Proceedings of the IEEE 25th Annual Power Electronics Specialists Conference, vol. 1, 1994, pp. 396–403.
[13] N. Patcharaprakiti, S. Premrudeepreechacharn, Y. Sriuthaisiriwong, Renew. Energy 30 (11) (2005) 1771–1788.
[14] T.L. Kottas, Y.S. Boutalis, A.D. Karlis, IEEE Trans. Energy Convers. 21 (3) (2006) 793–803.
[15] M.G. Simoes, N.N. Franceschetti, IEE Proc. Electr. Power Appl. 146 (5) (1999) 552–558.
[16] N. Ammasai Gounden, S.A. Peter, H. Nallandula, S. Krithiga, Renew. Energy 34 (3) (2009) 909–915.
[17] N. Ammasai Gounden, S.A. Peter, H. Nallandula, S. Krithiga, Energy 34 (2009) 909–915.
[18] T. Hiyama, S. Kouzuma, T. Imakubo, T.H. Ortmeyer, IEEE Trans. Energy Convers. 10 (3) (1995) 543–548.
[19] M. Veerachary, T. Senjyu, K. Uezato, IEEE Trans. Ind. Electron 50 (4) (2003) 749–758.
[20] I.H. Altas, A.M. Sharaf, Renew. Energy 33 (3) (2008) 388–399.
[21] D. Gao, Z. Jin, Q. Lu, J. Power Sources 185 (1) (2008) 311–317.
[22] M. Chaabene, M. Ben Ammar, A. Elhajjaji, Appl. Energy 84 (2007) 992–1001.
[23] MATLAB Simulink Simulation and Model Based Design User's Guide, Version 6.3 [Online]. Available: http://www.mathworks.com/access/helpdesk/help/pdf doc/simulink/sl using.pdf.
[24] M. Nikraz, H. Dehbonei, C.V. Nayar, A DSP-Controlled PV System with MPPT Australian Power Engineering Conference, Christchurch, 2003, pp. 1–6.
[25] Z.M. Salameh, M.A. Casacca, W.A. Lynch, IEEE Trans. Energy Convers. 7 (1) (1992), 93-.
[26] P. Siarry, F. Guely, Fuzzy Sets Syst. 99 (1) (1998) 37–47.
[27] E. Koutroulis, K. Kalaitzakis, N.C. Voulgaris, IEEE Trans. Power Electron 16 (1) (2001) 46–54.